The Astrophysical Journal, 540:1005–1015, 2000 September 10

TiO AND H_2O ABSORPTION LINES IN COOL STELLAR ATMOSPHERES

France Allard
CRAL (UML 5574) Ecole Normale Superieure, 69364 Lyon Cedex 7, France; fallard@ens-lyon.fr
Peter H. Hauschildt
Department of Physics and Astronomy and Center for Simulational Physics, University of Georgia, Athens, GA 30602-2451; yeti@hal.physast.uga.edu
and
David Schwenke
NASA Ames Research Center, Mail Stop 230-3, Moffett Field, CA 94035-1000; schwenke@pegasus.arc.nasa.gov
Received 1999 December 21; accepted 2000 March 29

ABSTRACT

We compare the structures of model atmospheres and synthetic spectra calculated using different line lists for TiO and water vapor. We discuss the effects of different line list combinations on the model structures and spectra for both dwarf and giant stars. It is shown that recent improvements result in significantly improved spectra, in particular, in the optical where TiO bands are important. The water vapor–dominated near-infrared region remains problematic as the current water line lists do not yet completely reproduce the shapes of the observed spectra. We find that the AMES TiO list provides more opacity in most bands and that the new, smaller oscillator strengths lead to systematically cooler temperatures for early-type M dwarfs than previous models. These effects combine and will help to significantly improve the fits of models to observations in the optical as well as result in improved synthetic photometry of M stars. We show that the Davis, Littleton, & Phillips f_{el}-values for the δ and φ bands of TiO best reproduce the observed $V-I$ color indices.

Subject heading: stars: atmospheres

1. INTRODUCTION

Over the past decade, model atmospheres and synthetic spectra for late-type stars have improved hand in hand with higher quality opacities. In 1994 quality lists of transitions of the water vapor molecule based on ab initio molecular calculations became available (Miller et al. 1994; Schryber, Miller, & Tennyson 1995; Jørgensen, Jensen, & Sørensen 1994), which allowed the computation of the first direct opacity sampling (hereafter dOS) model atmospheres for late-type dwarfs (Allard et al. 1994) and brown dwarfs (Allard et al. 1996), later to become the NextGen models described in Hauschildt, Allard, & Baron (1999a). Showing a more physical description of their main opacities, the NextGen dOS model atmospheres promised a better description of the spectral energy distribution (SED) of cool stars. And this appeared to be verified for the infrared SED of M dwarfs (Jones et al. 1996; Leggett et al. 1996; Allard et al. 1997).

But despite these fundamental improvements, the NextGen models have failed to match adequately several of the optical (spectroscopic and photometric) properties of late-type dwarfs and giants. In fact, the dOS models (Brett 1995; Allard et al. 1994, 1997; Hauschildt et al. 1999a) provided a worse fit to the optical SED of lower main-sequence dwarfs than previous models based on simplified molecular opacities (Allard & Hauschildt 1995, hereafter AH95). The models could not reproduce the tight relation formed by M dwarfs in the $V-R$ versus $R-I$ two-color diagram, indicating a systematically shallower slope of the optical SED (defined by TiO absorption) than observed in these stars. A systematic flux excess in the spectral region sampled by the V bandpass (0.4–0.65 μm) was noted as well in dwarfs as in red giants. Baraffe et al. (1998) observed that this excess in the NextGen dwarf models translated into lower main-sequence isochrones deviating progressively to the blue (by up to 1.0 mag!) in $V-R$ versus $R-I$ color-magnitude diagrams, for masses lower than about 0.5 $M_\odot$ ($T_{eff} \leq 3800$ K). Baraffe et al. (1997) examined a variety of globular clusters and showed that this departure of the models decreased in amplitude with decreasing metallicity. The problem seemed therefore confirmed to be caused by a lack of opacity of an oxygen compound.[1]

Only three independent models of the TiO molecule and corresponding lists of transitions were available so far to the construction of model atmospheres. The first model was constructed over two decades ago by Collins (1975) and was restricted by the computational limitations of the time. The Collins line list was intended to model the extended atmospheres of red giants and did not include high-energy and otherwise weak transitions important by their number in the hotter environments of red dwarf atmospheres. It also neglected the red ϵ system of TiO. Jørgensen (1994) extended Collins's work to TiO isotopic transitions, included the ϵ system from revised molecular rotational constants, and adopted the laboratory oscillator strengths of Davis, Littleton, & Phillips (1986). It is therefore understandable that the resulting limited list of transitions caused shortcomings in the NextGen model atmospheres. The second TiO list was constructed by Kurucz (1993) and is used in his ATLAS9-12 atmospheres. The third model was constructed by Plez (1992) using also the Davis et al. (1986) oscillator strengths and is used in his version of the MARCS atmosphere code. All three independent models yielded the visual flux excess in different proportions. Plez (1998) suggested that the missing opacity is due to missing TiO band systems in current lists and added the TiO a–f system at 0.5

[1] Hydride absorption bands only get stronger relative to the continuum with decreasing metallicity over the range covered by the globular clusters studied in Baraffe et al. (1997) in the optical spectral range.

μm to his list. However, this helped him only partially to resolve the V-band flux excess problem.

Recently, Langhoff (1997) constructed a new model of the TiO molecule and published new lifetimes and oscillator strengths that improved significantly upon the 1986 values of Davis et al. (Valenti, Piskunov, & Johns-Krull 1998; Plez 1998). Schwenke (1998) has subsequently computed a corresponding list of transitions complete to the high energies and therefore more suitable for general model atmosphere applications. In this paper we present the results of including this new TiO line list as well as the new AMES-H_2O list in the construction of model atmospheres and synthetic spectra for late-type dwarfs and red giants.

2. MODEL CALCULATIONS

We have calculated the models presented in this paper using version 10.3 of our general model atmosphere code PHOENIX. Details of the code and the general input physics are discussed in Hauschildt et al. (1999a) and references cited therein. The models for M giants were calculated with the same setup; however, they employ spherical geometry (including spherically symmetric radiative transfer). For giant models with low gravities $\log g \leq 3.5$, this can be an important effect for the correct calculation of the structure of the model atmosphere and the synthetic spectrum (Aufdenberg et al. 1998, 1999). The main difference between the models presented in Hauschildt et al. (1999a) and the models presented here is the use of the new AMES line lists for H_2O (Partridge & Schwenke 1997) and TiO (Schwenke 1998), but we have also adjusted the empirical oscillator strengths of VO and CaH absorption bands to respect their strength relative to TiO bands (note that VO and CaH absorption is still treated in the just overlapping line approximation because of the lack of adequate line data). Our combined molecular line list includes about 500 million molecular lines. These lines are treated with a dOS technique where each line has its individual Voigt (for strong lines) or Gauss (weak lines) line profile (in the standard OS method, tables of precomputed opacities are used). They are selected for every model from the master line list to the beginning of each model iteration to account for changes in the model structure; see Hauschildt et al. (1999a) for details. This procedure selects about 215 million molecular lines for a typical giant model with $T_{\rm eff} \approx 3000$ K and about 130 million molecular lines for a dwarf model with the same effective temperature. Therefore, we generally use the parallelized version of PHOENIX (Hauschildt, Baron, & Allard 1997; Baron & Hauschildt 1998; Hauschildt & Baron 1999) to perform the calculation efficiently on parallel supercomputers. Details of the TiO and H_2O lists are given in the next subsections.

2.1. *Water Lines*

The effects of water lines on the M-dwarf SED was discussed in Allard et al. (1994). For the work presented here, we have replaced the UCL water vapor line list (Miller et al. 1994; Schryber et al. 1995; hereafter MT-H_2O) used in Hauschildt et al. (1999a) with the AMES water line list (Partridge & Schwenke 1997; hereafter AMES-H_2O). This list includes about 307 million lines of water vapor. For the calculations shown in this paper, we have used $H_2^{16}O$ and neglected other, much less abundant, isotopes of this molecule.

The water vapor opacity is governed by the completeness of the line list used but also by the adopted atomization energy. The partition function of the molecule cancels out in the final absorption coefficient, after we have multiplied cross sections by number densities. But since water is an important chemical equilibrium species, errors in the partition function can affect indirectly the model structure and spectra. The AH95 models were based on the Ludwig (1971) hot flames water cross sections in the form of straight means and used the JANAF partition function for water vapor (Irwin 1988). The NextGen models were, on the other hand, computed with the MT-H_2O line list and a partition function computed from the MT-H_2O levels. We note that the AMES-H_2O partition function is practically identical to JANAF values, while the MT-H_2O value is smaller than JANAF for temperatures above 3000 K, possibly due to the energy levels missing in the MT-H_2O data. We have therefore adopted for this and later work the JANAF partition function. We use an atomization energy of 9.5119 eV from Irwin (1988) for all models since AH95.

2.2. TiO *Lines*

The main point of this paper is the comparison of the model structure and the synthetic spectra obtained by using the list of TiO lines from Jørgensen (1994; hereafter SCAN-TiO) and the new list of TiO lines from Schwenke (1998; hereafter AMES-TiO). The AMES-TiO list includes a total of about 172 million lines; about 44.6 million of these are for the most abundant isotope ^{48}TiO and about 32 million lines for each of the remaining four isotopes (^{46,47,49,50}TiO). TBut beyond the completeness of the line list, two more considerations affect the overall opacity produced by TiO and explain systematic differences between model versions and by different authors: the atomization energy (D_0^0) determines the number density of TiO, and the TiO band oscillator strengths[2] have been derived from sunspot observations (Davis et al. 1986, hereafter DLP86), laboratory experiments (Hedgecock, Naulin, & Costes 1995, hereafter HNC95), as well as from ab initio calculations (Langhoff 1997, hereafter L97). Brett (1990, hereafter B90) derived astrophysical $f_{\rm el}$-values by fitting the optical SEDs of red giants, using an atomization energy of 7.76 eV. He quoted that reducing this value by 0.3 eV would increase his $f_{\rm el}$ by a factor of 2.5. The most recent estimate of D_0^0 for TiO is now 6.92 eV, which suggests that the B90 $f_{\rm el}$-values are underestimated by as much as a factor of 7! We summarize in Table 1 the various sources of oscillator strengths available for TiO.

The models of Allard (1990) used $f_{\rm el}$-values from B90 together with the straight mean TiO opacities by Collins (1975) and Collins & Faÿ (1974) and assuming an atomization energy of 6.87 eV. The first comparison of these models to the SED of M dwarfs (Kirkpatrick et al. 1993) revealed the inadequacy of this combination of parameters for TiO, which produced far too weak optical opacities. We have therefore, since the AH95 model series, employed the updated value of 6.92 eV together with the larger laboratory $f_{\rm el}$-values of DLP86. These two modifications combined to significantly increase the strength of TiO opacities in the models, bringing the AH95 and later the dOS NextGen models in improved agreement with the SED of M dwarfs.

[2] $f_{\rm el} = f_{v'v''}/q_{v'v''}$, where the f's are the oscillator strengths and the q's are the Franck-Condon factors of the transition $v'v''$.

TABLE 1

TiO f_{el} VALUES ($f_{el} = f_{v'v''}/q_{v'v''}$)

System	λ_0 (Å)	B90	J94[a]	DLP86	L97	AP98	Adopted
α	5170.7	0.10	0.17	0.106	0.105	0.106	0.105
β	5605.2	0.15	0.28	0.125	0.176	0.125	0.176
γ'	6192.5	0.08	0.14	0.0935	0.108	0.0935	0.108
γ.......	7095.8	0.09	0.15	0.0786	0.092	0.0786	0.092
ϵ.......	8407.6	0.0024	0.014	<0.006	0.002	0.0023	0.002
δ	8870.9	0.02	0.048	...	0.096	0.048	0.048
ϕ	11044.8	0.02	0.052	...	0.018	0.0178	0.052

[a] Laboratory values determined by HNC95.

REFERENCES.—B90: Brett 1990; DLP86: Davis et al. 1986; J94: Jørgensen 1994; HNC95: Hedgecock et al. 1995; L97: Langhoff 1997; AP98: Alvarez & Plez 1998.

Any differences in the predictions of the AH95 and NextGen models are therefore purely due to the opacity technique (straight mean vs. dOS) and to the completeness of the line list used. The incompleteness of the SCAN-TiO line list allows photons to escape between absorption bands (see, e.g., Valenti et al. 1998) and thus leads to systematically and increasingly (with higher T_{eff}) bluer optical colors $V-I$ than observed (Baraffe et al. 1997, 1998). For the current models we therefore explore the use of the more complete AMES-TiO line list and the yet larger theoretical f_{el}-values of L97.

3. RESULTS

We have calculated a number of model atmospheres using either the SCAN-TiO or the AMES-TiO list of TiO lines and using either AMES-H_2O or MT-H_2O as source of the H_2O lines. All the other input physics are the same for both sets of models. All models have been fully converged with their respective set of parameters. Note that these models have been constructed for the purpose of this paper only and not to model individual stars and thus do not include dust formation and opacities, which is important in atmosphere models with effective temperatures below about 2500 K; such models will be presented in a subsequent paper. In the following, we discuss the results for the dwarf and giant models separately. The baseline for our comparisons are the NextGen models (Hauschildt et al. 1999a) for the dwarfs and the NG-giant models (Hauschildt et al. 1999b) for the giants.

3.1. *Effects of Different* TiO *Line Lists*

The models discussed in this section were all calculated using AMES-H_2O to isolate the effects of different TiO line lists on the model spectra and structures.

3.1.1. *M-Dwarf Models*

In Figures 1 and 2 we show a comparison of model spectra calculated with AMES-TiO (*solid curves*) and with SCAN-TiO (*dotted curves*) (both using our adopted f_{el} set, as quoted in Table 1) for several effective temperatures. The gravity ($\log g = 5.0$) and abundances (solar) were selected to be representative of M dwarfs in the solar neighborhood. In both figures, the resolution of the synthetic spectra was reduced by boxcar smoothing to 20 Å. At high effective temperatures, the two sets of models are nearly identical due to reduced importance of TiO absorption. At very low T_{eff} the two line lists apparently agree very well since only the lowest levels of TiO remain populated. It is essentially between $T_{eff} \approx 2000$ and ≈ 3500 K that the largest completeness and quality effects of the TiO line lists are seen.

Figure 3 indicates the location of each TiO band system for a 2900 K model. From this it becomes clear that the addition of a–f transitions, which depress the continuum from 0.4 to 0.5 μm, is one of the largest improvements brought by the AMES-TiO list to our models. We note that the entire optical regime from 0.4 to 0.75 μm shows generally *more* opacity in the AMES-TiO models than using the Jørgensen (1994, hereafter J94) line list. The ϵ bands at 0.82–0.88 μm have a more precise shape in the AMES-TiO list and come out stronger as well. This is a result of the completeness of the AMES-TiO list, which also removes flux excess escaping between the troughs of the bands. We note however that some regions, such as the γ-band near 0.78 μm, show less opacity in the new models.

The main effect of the new AMES-TiO on spectroscopic and photometric T_{eff} estimates will, however, be dominated by the change we make to the oscillator strengths. The L97 f_{el}-values being generally smaller than the DLP86 values adopted by J94, models of early-type M dwarfs using the new AMES-TiO setup should predict systematically lower effective temperatures than did prior models (NextGen, AH95, etc.; see also Fig. 10 below). And beyond the enhanced completeness of the AMES-TiO list to high temperature transitions, the need for a cooler model should also contribute to making the TiO bands fit better a given star, i.e., larger bands with less flux escaping from deeper, hotter atmospheric regions between them.

We could have opted to use the HNC95 laboratory f_{el}-values as did Plez (1998), but since the L97 ab initio values agree quite well, we decided to keep these, except for the δ- and φ-band systems. The reason the oscillator strengths for the δ and φ bands are less accurate is that it is very hard to get a good description of the b state, which is the upper state in both bands. For the δ system, L97 derives an oscillator strength which is, as opposed to all other bands, twice as large as the DLP86 value. And the δ and φ f_{el}-values cannot be corroborated by recent experimental values. Such a strong δ-band system would be difficult to bring in agreement with M-dwarf observations. Indeed, prior models have all shown a gradually increasing departure to the blue of the main sequence in M_V versus $V-I$ diagrams (Baraffe et al. 1995, 1998). Such departure is significantly improved using the new TiO list if one keeps a weak δ band as indicate preliminary results of evolution models to be published separately (see also Fig. 12 below). We have therefore adopted to keep the DLP86 oscillator strength values for

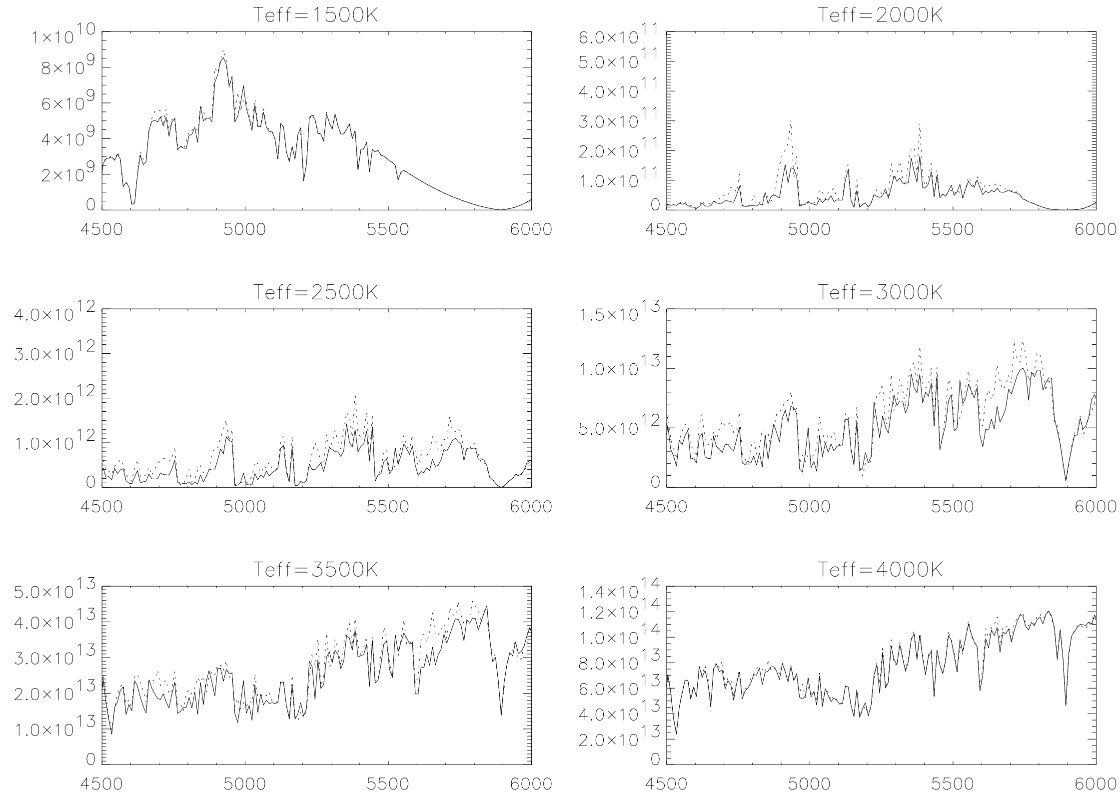

FIG. 1.—Comparison between solar abundance M-dwarf models calculated using AMES-TiO (*solid curves*) and SCAN-TiO (*dotted curves*) in the blue spectral region.

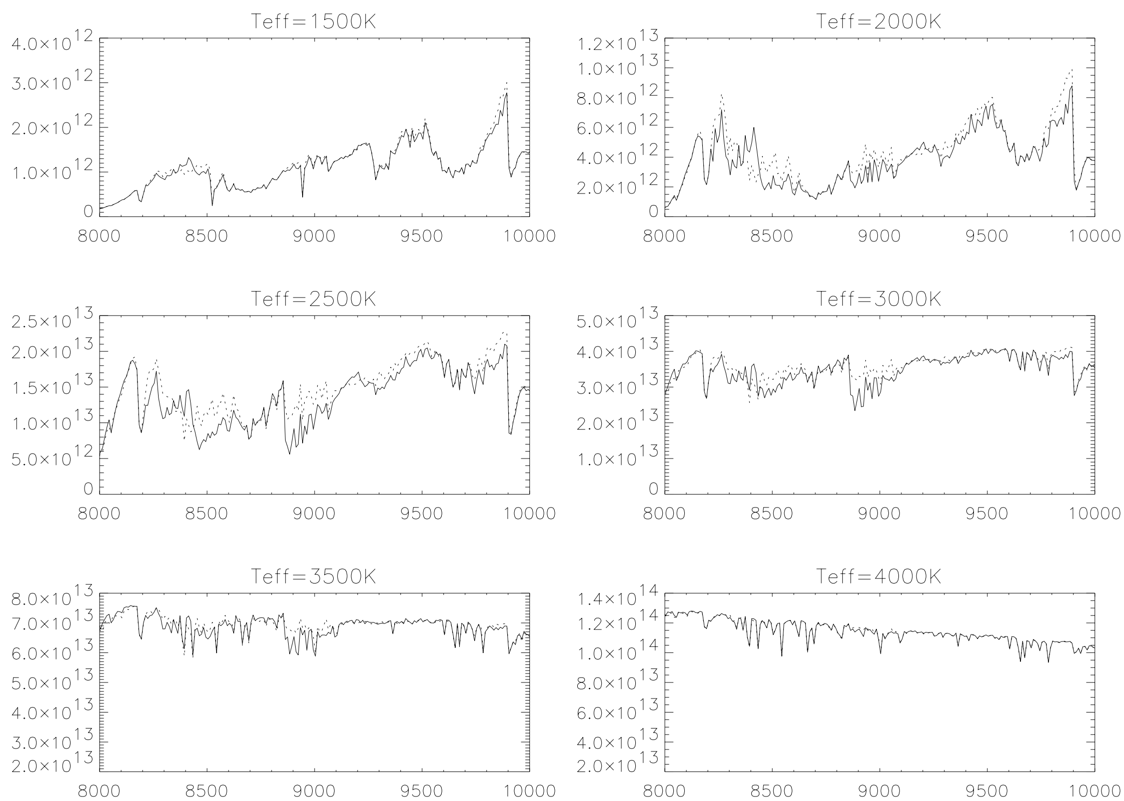

FIG. 2.—Comparison between solar abundance M-dwarf models calculated using AMES-TiO (*solid curves*) and SCAN-TiO (*dotted curves*) in the red spectral region.

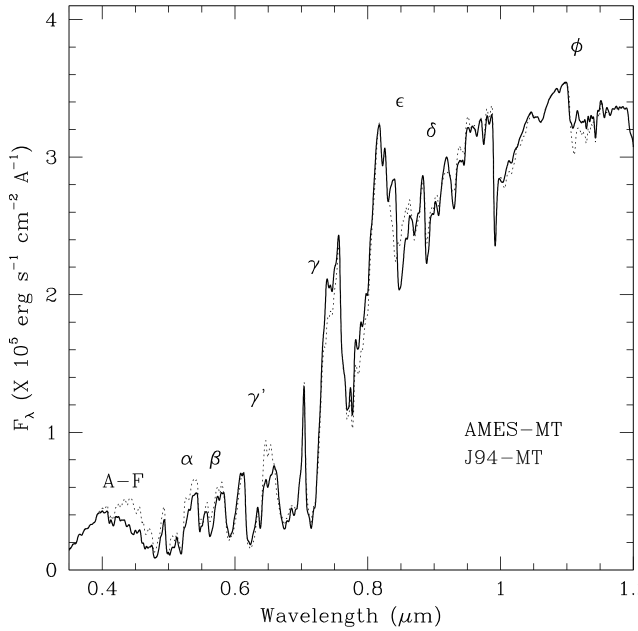

FIG. 3.—Comparison among $T_{\rm eff} = 2900$ K, $\log g = 5.0$, and solar abundance (M/H = 0.0) models calculated using AMES-TiO (*solid curves*) and SCAN-TiO (*dotted curves*) based on the same set of TiO oscillator strengths (see "Adopted" in Table 1). The models use otherwise identical opacities and parameters. Each model is fully converged, and the synthetic spectra are downgraded to a resolution of 20 Å. The positions of the TiO band heads are indicated according to Table 8 of Langhoff (1997).

the reddest two TiO bands until new laboratory experiments can either confirm or refute the L97 predictions. The summary of our adopted set of oscillator strengths for TiO is presented in Table 1.

3.1.2. *M-Giant Models*

The results for the giant models are similar to the results for the dwarfs. Figures 4 and 5 show synthetic spectra for three representative giant models with the indicated effective temperatures. The models have in common the parameters $\log g = 0.5$, $M = 5\ M_\odot$, and solar abundances. The differences between the AMES-TiO (*solid curves*) and SCAN-TiO (*dotted curves*) models are somewhat larger for giants than for the dwarfs in the blue spectral region due to an increased sensitivity to the added a–f system opacities in the AMES-TiO line list. It is however somewhat less pronounced in the red spectral region where TiO bands are weaker in giants. The "spikes" that are apparent in the SCAN-TiO spectrum with $T_{\rm eff} = 3000$ K are absent in the AMES-TiO models. These spikes were one of our major problems in fitting observed spectra of giants. For larger $T_{\rm eff}$ the differences between the spectra diminish quickly as TiO becomes less important in the giants. This happens at lower effective temperatures compared to the dwarfs because of the lower pressures in giant atmosphere, which result in smaller partial pressure of molecules as compared to dwarfs.

3.1.3. *Model Structures*

A comparison of the model structures for both dwarfs and giants reveals only very small differences between structures calculated with AMES-TiO and SCAN-TiO. We plot the differences in electron temperature as well as the relative differences between the AMES-TiO and SCAN-TiO models for dwarfs and giants in Figures 6 and 7, respectively. The changes are generally very small, only in the percent range for the gas pressures and about 10 K maximum difference between the electron temperatures for the dwarf models.

FIG. 4.—Comparison between solar abundance M-giant models calculated using AMES-TiO (*solid curves*) and SCAN-TiO (*dotted curves*) in the blue spectral region.

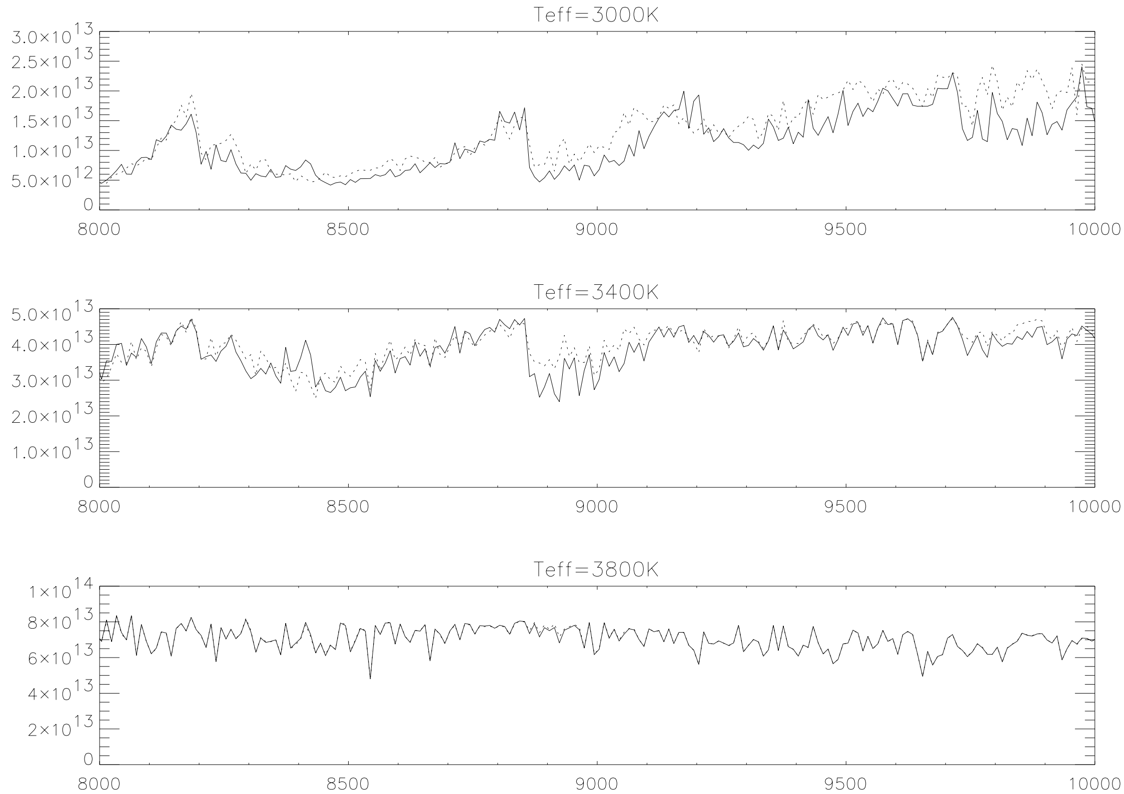

FIG. 5.—Comparison between solar abundance M-giant models calculated using AMES-TiO (*solid curves*) and SCAN-TiO (*dotted curves*) in the red spectral region.

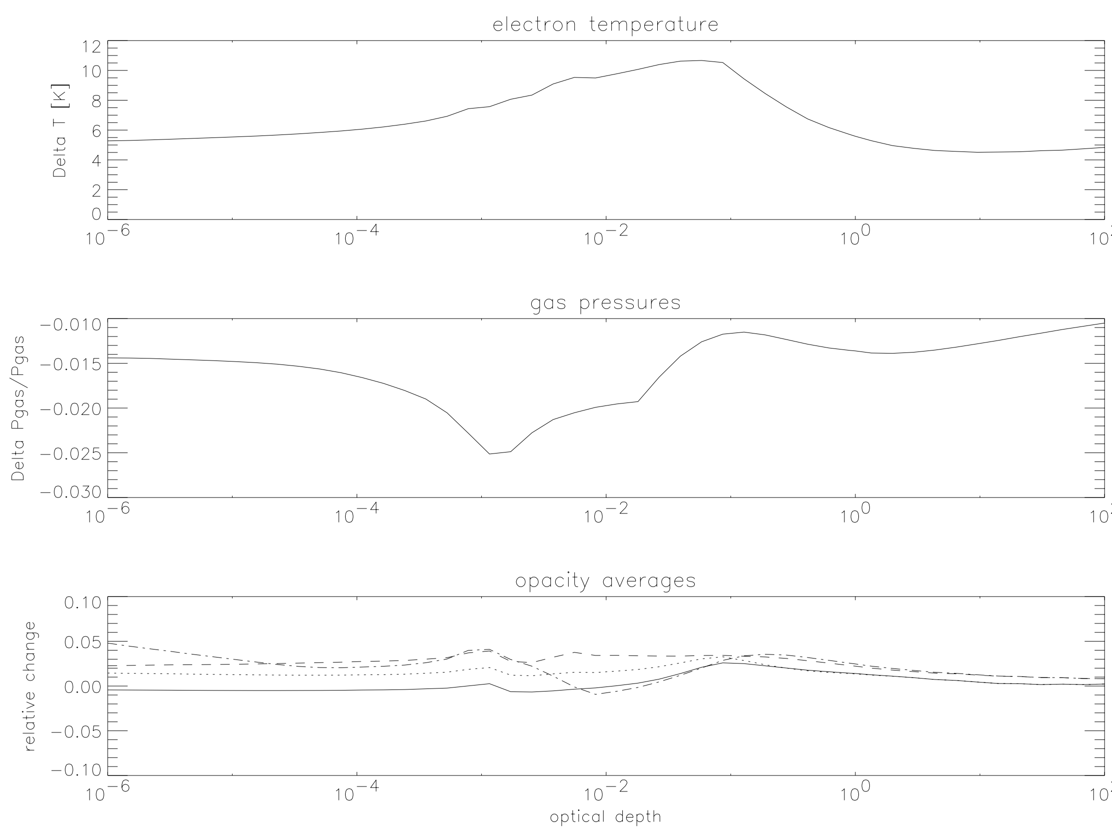

FIG. 6.—Comparison between solar abundance M-dwarf models with $T_{\rm eff} = 2500$ K calculated using AMES-TiO and SCAN-TiO. The differences are calculated in the sense AMES-TiO minus SCAN-TiO model. The bottom panel gives the results for the Planck (*solid curve*), *J* (*dotted curve*), flux (*dashed curve*), and Rosseland (*dot-dashed curve*) mean opacities.

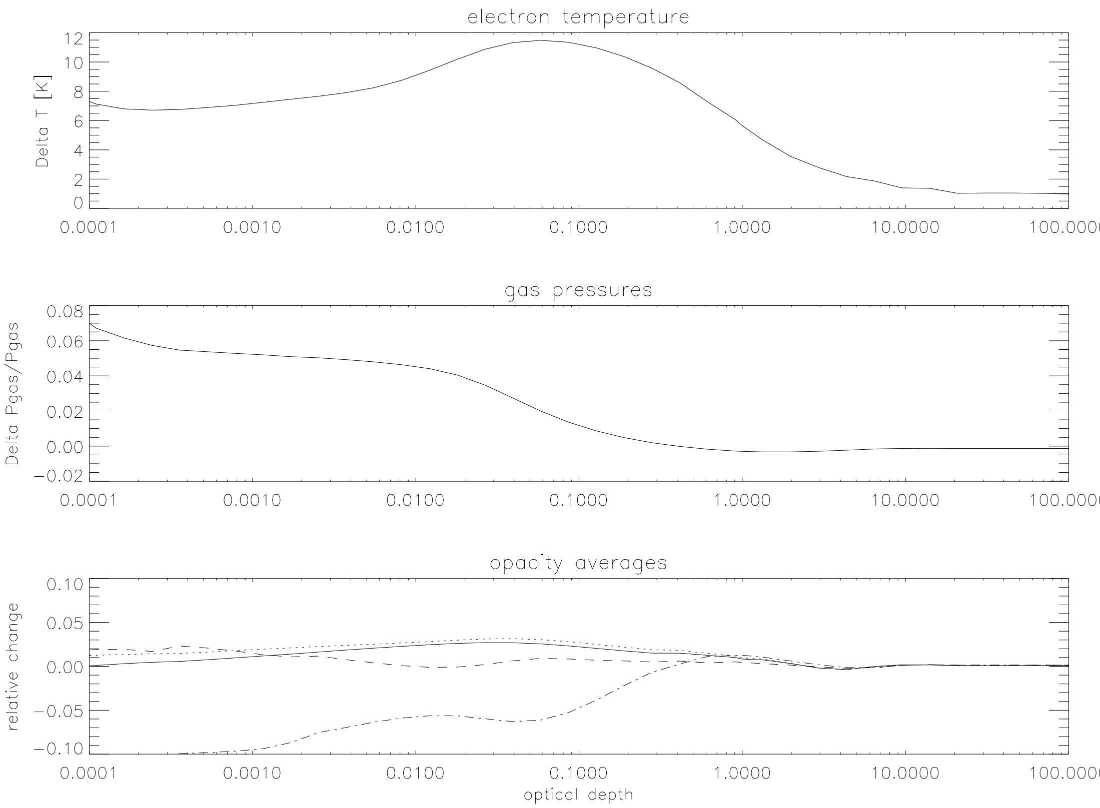

FIG. 7.—Comparison between solar abundance M-giant models with $T_{eff} = 3000$ K calculated using AMES-TiO and SCAN-TiO. The differences are calculated in the sense AMES-TiO minus SCAN-TiO model. The bottom panel gives the results for the Planck (*solid curve*), *J* (*dotted curve*), flux (*dashed curve*), and Rosseland (*dot-dashed curve*) mean opacities.

For the giant models the differences are somewhat larger. The changes in the opacity averages are generally small but largest for the Rosseland mean opacity in the outer layers of the giant models. The temperatures are higher in the AMES-TiO model for both the giant and the dwarf models; however, the gas pressures are lower in the AMES-TiO dwarf model but higher in the AMES-TiO giant model. Overall, the changes are modestly small, indicating that the detailed effects of the TiO line lists do not have a large effect on the model structure itself.

3.2. *Effects of Different Water Vapor Line Lists*

In Figure 8 we show the effects of different water line lists on the synthetic spectra for M dwarfs. All models shown in the graph otherwise use the same line lists (AMES-TiO was used for the TiO lines). Overall, we can see that the changes in the water vapor line lists are of larger amplitude than the changes in the completeness of the TiO line list. The models calculated with AMES-H_2O show a totally different shape of the 1.4 μm band, both weaker and wider than predicted by the MT-H_2O model. The completeness of the new line list to high temperatures helps block more flux escaping from deeper, hotter layers of the models around 1.6 and 2.2 μm. This promises a much better description of observations in general.

We also find important changes of the model structure as shown in Figure 9. The differences of the electron temperatures can reach 100 K; the gas pressures can differ by 20; and the opacity averages, in particular, the Rosseland mean, can differ by close to 60%. These effects are much larger in the outskirts of the atmosphere than the changes in the structures caused by different TiO line lists (see Fig. 6). As a result, the use of the AMES-H_2O line list also affects the optical spectra, causing weaker TiO bands than obtained with the MT-H_2O line list. Models of early-type M dwarfs based on the AMES-H_2O line list therefore systematically predict yet lower effective temperatures for a given star.

3.3. *Combined Effects*

In Figures 10 and 11 we display a comparison between NextGen models (which use MT-H_2O and SCAN-TiO) and models that use the AMES-H_2O and AMES-TiO. The wavelength range of important filters and band identifications for TiO are given on the figures. The TiO bands in the "AMES atmosphere" are considerably weaker than those of the NextGen model spectrum as a result of the smaller oscillator strengths used and the structural effects. On the other hand, the water bands are stronger in the AMES atmosphere than in the NextGen model. This model has a relatively high temperature; thus, the higher energy levels of the water molecule are relatively more important than for models with lower T_{eff} (however, the concentration of water molecules is reduced so the overall water opacity is smaller than in the cooler models).

To better judge the impact of these opacity changes on the overall SED of M dwarfs in general, we have computed synthetic photometry as described in AH95 for three sets of models: (1) the NextGen grid based on J94 and MT-H_2O, (2) the AMES grid based on AMES-TiO and AMES-H_2O opacities, and (3) the AMES-MT grid based on AMES-TiO and MT-H_2O opacities. The results are compared to a

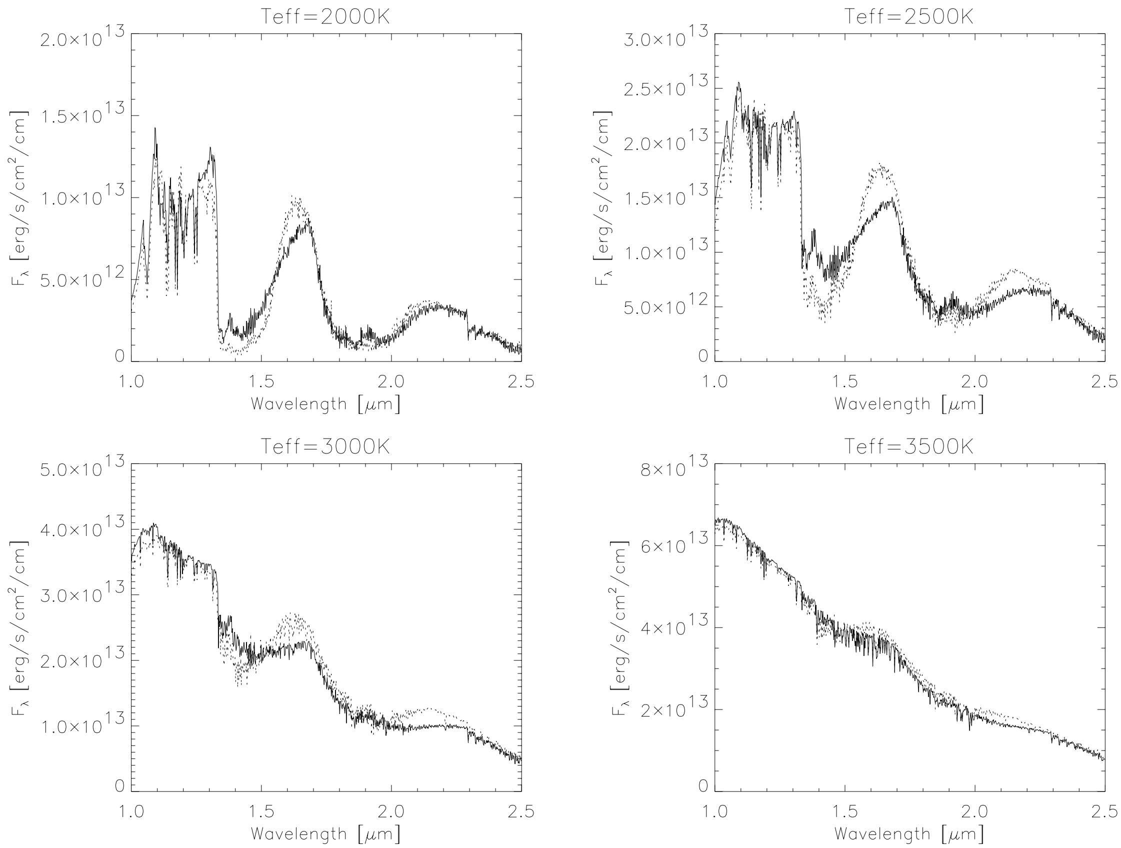

FIG. 8.—Comparison between solar abundance M-dwarf models calculated using AMES-H_2O (*solid curves*) and MT-H_2O (*dotted curves*) in the near-infrared spectral region. Both sets of models were calculated using AMES-TiO and iterated to convergence with their respective parameters.

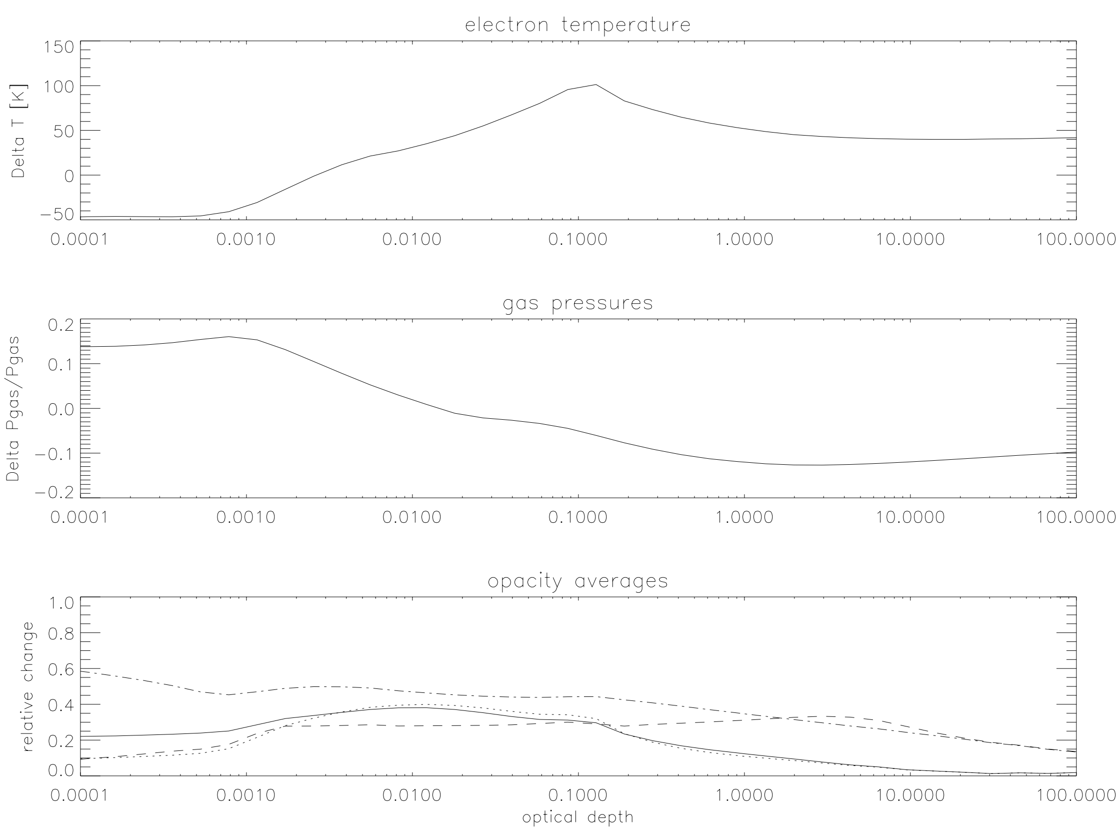

FIG. 9.—Comparison between solar abundance M-dwarf models with $T_{\rm eff} = 2500$ K calculated using AMES-H_2O and MT-H_2O. The differences are calculated in the sense AMES-H_2O minus MT-H_2O. The bottom panel gives the results for the Planck (*solid curve*), J (*dotted curve*), flux (*dashed curve*), and Rosseland (*dot-dashed curve*) mean opacities. Both sets of models were calculated using AMES-TiO and iterated to convergence with their respective parameters.

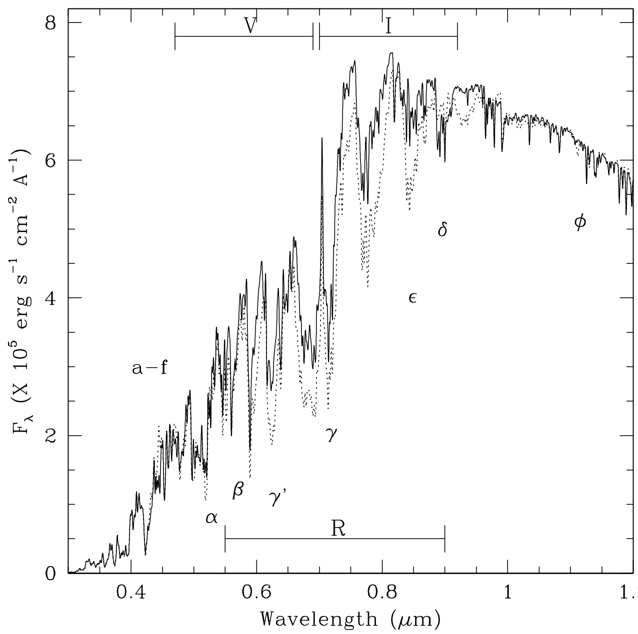

FIG. 10.—We compare the optical spectral distribution of a NextGen model with $T_{\rm eff} = 3500$ K, log $g = 5.0$, [M/H] = 0.0 (*dotted line*) with a model converged on the same parameters using the AMES-TiO and H_2O line lists (*solid line*). The positions of the TiO band heads are indicated according to Table 8 of Langhoff (1997). The region of integration of standard optical broadbands is also shown for reference. The "AMES atmosphere" shows weaker TiO bands, principally due to the smaller oscillator strengths predicted by the Langhoff TiO model.

photometric sample of M dwarfs (Leggett 1992) in Figures 12, 13, and 14. Since M dwarfs form a tight sequence in the optical *VRI* two-color diagram despite the age and metallicity scatter of the sample (see AH95), this diagram imposes a strong constraint on model atmospheres. We find that models based on AMES-TiO opacities are systematically redder in $V-R$ and $V-I$ than models based on the J94 line list. The new models agree much better with observations, and the new TiO data removes most of the discrepancy shown by the NextGen models in the lower main sequence. Small remaining discrepancies may be attributed to the JOLA handling of VO and CaH, which tends to overestimate slightly their opacities in the present models. Leinert et al. (2000) already studied the low-resolution *Hubble Space Telescope*/Faint Object Spectrograph spectra of an M6 dwarf (LHS 1070A) and found the AMES-MT models indeed agree quite well both with the observed SED and

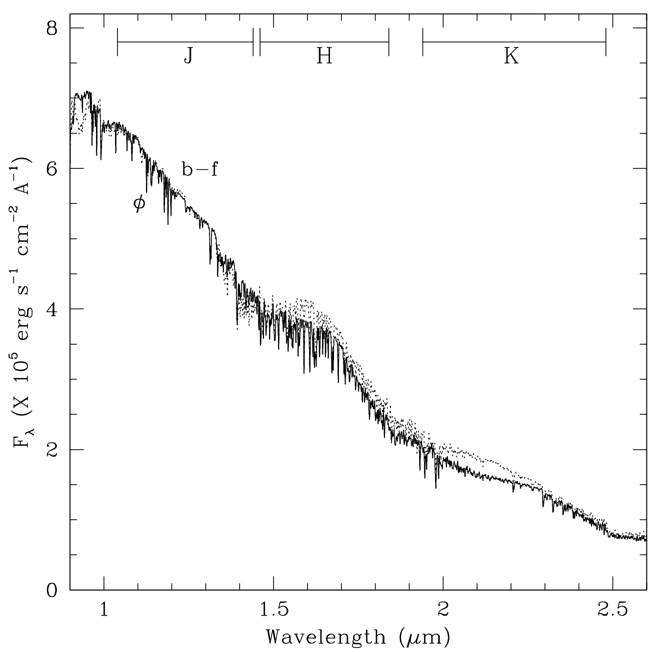

FIG. 11.—Same as in Fig. 10 for the near-infrared portion of the spectrum. The region of integration of the standard near-infrared broadbands are also shown for reference. The "AMES atmosphere" shows stronger H_2O bands, especially in the trough of the bands, i.e., at 1.6 and 2.1 μm. But little or no changes are seen in the *J* bandpass region.

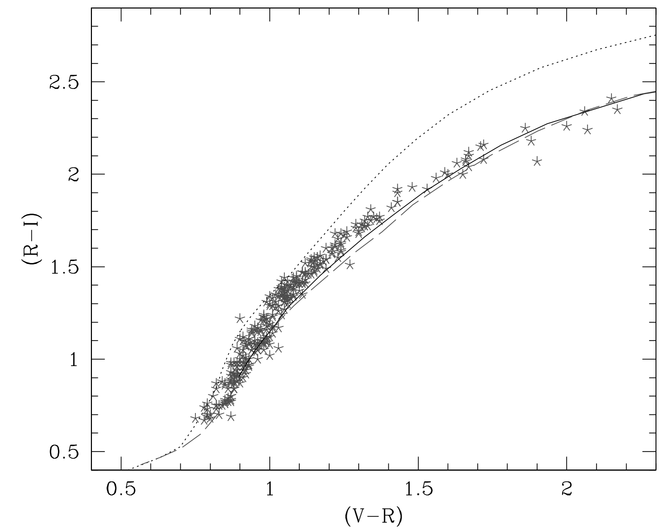

FIG. 12.—Optical Cousins broadband synthetic photometry of solar metallicity and fixed gravity (log $g = 5.0$) models of the NextGen grid (*dotted line*), AMES-MT grid (*long-dashed line*), and AMES grid (*solid line*) are compared to the photometric sample of Leggett (1992). This sample contains mostly M dwarfs and metal-depleted M subdwarfs of the solar neighborhood and becomes scarce in the late-type dwarf regime.

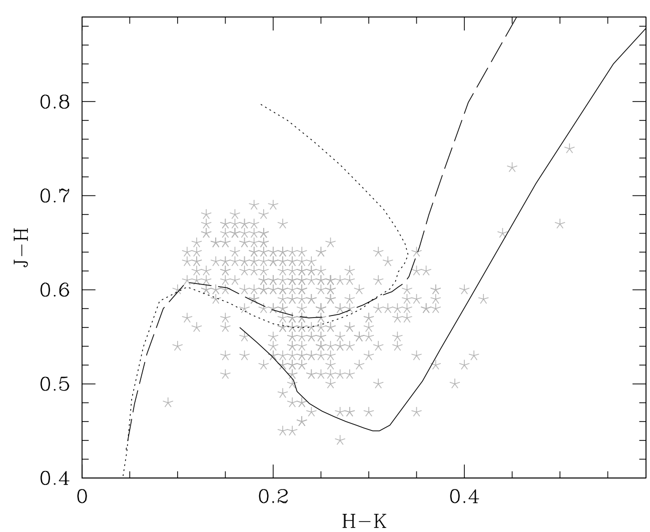

FIG. 13.—Same as Fig. 12 for near-infrared broadband colors covering the water opacity range. Please note that the hot star tail of the sample, near $H-K = 0.1$, is reproduced by the NextGen and AMES-MT models for the lower gravities predicted by evolution models for 5–10 Gyr isochrones. Of the models shown, only the NextGen are grainless, which explains their curling up at the low-temperature end compared to AMES-MT models.

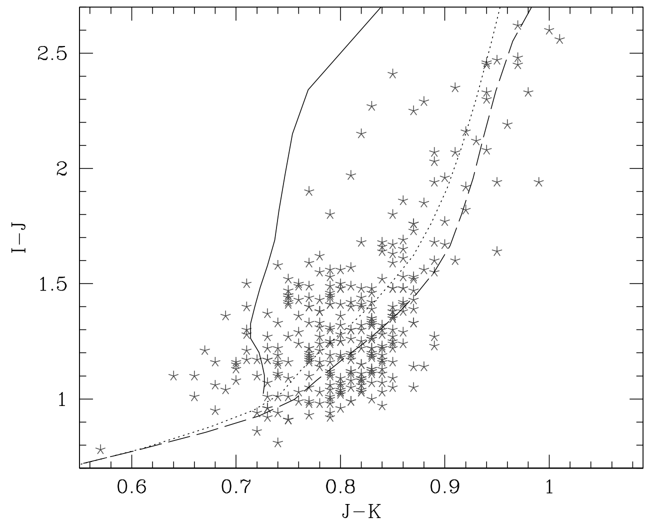

FIG. 14.—Same as Figs. 12 and 13 for broadband colors sampling side to side of the SED's flux peak.

absolute fluxes within errors on the parallax of the system. They however noticed that some "continuum" flux excess remains important in the visual part of the SED (0.45–0.65 μm). However, there is no a priori reason to assume that the a–f oscillator strengths are inaccurate, and these remaining problems could be related to other effects on the model structure.

The use of AMES-H_2O seems also to bring some improvements to the modeling of near-infrared colors. Figure 13 shows that the late-type dwarfs can be better reproduced by the new water opacities than by the MT-H_2O line list. However, this diagram is sensitive to both gravity (lower gravity models loop lower) and metallicity, which makes it difficult to constrain the models on the adequacy of the water opacities used with them. Leggett, Allard, & Hauschildt (1998) and Leggett et al. (2000) have already used the AMES models in their analysis of M dwarfs and brown dwarfs and found an excellent general agreement of the predicted near-infrared SED with observations. However, these analyses used the models to derive the parameters of the studied stars and brown dwarfs based on fits to the near-infrared SED or photometry and could not make an independent statement on the quality of the water line list.

M dwarfs form again a sequence in the mixed-color IJK diagram (Fig. 14), although less tightly than in the VRI diagram. Unresolved binary stars produce K-band flux excess and lie below the sequence. H_2 pressure–induced opacities depress the K-band flux of metal-depleted dwarfs so that they systematically lie above the sequence. But, as opposed to the JHK diagram, this one is not particularly sensitive to gravity in M dwarfs, which allows a sequence to be defined. Models should pass, therefore, through the bulk of early-type M dwarfs at $J-K=0.8$ and follow a relatively $J-K$–insensitive sequence toward late-type dwarfs. We find that models based on the AMES-H_2O opacities lie, as did the AH95 models before them, 0.2 mag in $J-K$ to the blue of the observed sequence! And our tests show that this result is independent of the TiO opacities used. The NextGen models already reproduced perfectly the location of lower main-sequence stars in this diagram. And AMES-MT models computed using the AMES-TiO and MT-H_2O line lists behave adequately both in the optical and infrared. Why? Perhaps the new water vapor line list is still not complete enough to high temperatures and lacks opacity in the J bandpass, i.e., around 1.3 μm? Or would it have too much opacity in the K window, i.e., around 2.2 μm? Until these questions can be answered, we hope that the two main grids of models we have computed (AMES and AMES-MT) will allow independent detailed confrontations to observations of cool stars that will locate more precisely the source of the problem (e.g., Leinert et al. 2000 in preparation).

4. SUMMARY AND CONCLUSIONS

A long-standing problem with M-dwarf models was that prior TiO line lists were incomplete to high temperatures. The use of "straight means" (AH95 models) helped by the coarseness of the treatment to block flux that otherwise escapes between lines in the incomplete list. But these models also blocked too much flux in most cases and were only appropriate in late-type M dwarfs when TiO bands are already very strong. Clearly, a more complete line list was needed to model stars from the onset of TiO formation to its gradual disappearance from the gas phase in brown dwarfs. The AMES-TiO list now serves beautifully this purpose. We find that the list provides more opacity in most bands and suppresses adequately flux between bands. The new, smaller oscillator strength values also play an important role in systematically assigning cooler models (at least for early-type M dwarfs) to a given star, this way contributing to broader bands and lesser interband flux as well. These effects combine and should resolve most of the previously observed discrepancy between models and observations in the optical SED and photometry of M stars. Leinert et al. (2000) note, however, that flux excess remains substantial in the visual spectrum, suggesting some further incompleteness or f_{el} inaccuracies of the new TiO in the a–f system.

In order to better reproduce the observed $V-I$ color indices, we had to retain in the present models the Davis et al. (1986) f_{el}-values for the two reddest band systems: δ and φ. For these two band systems, the theoretical estimates of Langhoff (1997) predict an unexpectedly large f_{el}-value ratio, while no laboratory estimates (Hedgecock et al. 1995) are available to corroborate this. And we find, as did Alvarez & Plez (1998) in red giants for the δ-band, that models based upon the DLP86 f_{el}-values for these two bands reproduce adequately their observed depths in M dwarfs.

The introduction of the AMES-H_2O opacities brings solid improvements of the near-infrared SED of late-type dwarfs but fails as the AH95 models did to reproduce adequately the $J-K$ colors of hotter stars. Water vapor is a more important factor for the structure of the atmosphere than TiO because its overall opacity is larger and its lines are closer to the peak of the SED than the TiO bands, so the flux-blocking effect of water vapor is more important for the temperature structure than that of TiO opacities for these low temperatures. Schwenke and collaborators at NASA AMES are preparing a new dipole moment function for H_2O, which may change the high-temperature, high-overtone water bands and help resolve this discrepancy in the near future.

Until a revised version of the AMES-H_2O line list becomes available, we have therefore generated two sets of model atmospheres for cool stars that allow investigation of these issues: the AMES grid based on the new TiO and H_2O opacities and the AMES-MT grid that relies on the AMES-TiO and MT-H_2O opacities.

We thank David Alexander for helpful discussions and the referee, U. G. Jørgensen, for his very helpful comments. This work was supported in part by grants from CNRS and INSU, NSF grant AST 97-20704, NASA ATP grant NAG 5-3018 and LTSA grant NAG 5-3619 to the University of Georgia, and NASA LTSA grant NAG 5-3435 to Wichita State University. This work was supported in part by the Pôle Scientifique de Modélisation Numérique at ENS-Lyon. Some of the calculations presented in this paper were performed on the IBM SP2 of CNUSC, on the SGI Origin 2000 of the UGA UCNS, on the IBM SP2 of the San Diego Supercomputer Center (SDSC) with support from the National Science Foundation, and on the Cray T3E of the NERSC with support from the DoE. We thank all these institutions for a generous allocation of computer time.

REFERENCES

Allard, F. 1990, Model Atmospheres for M Dwarfs, Ph.D. thesis, Univ. Heidelberg
Allard, F., & Hauschildt, P. H. 1995, ApJ, 445, 433 (AH95)
Allard, F., Hauschildt, P. H., Alexander, D. R., & Starrfield, S. 1997, ARA&A, 35, 137
Allard, F., Hauschildt, P. H., Baraffe, I., & Chabrier, G. 1996, ApJ, 465, L123
Allard, F., Hauschildt, P. H., Miller, S., & Tennyson, J. 1994, ApJ, 426, L39
Alvarez, R., & Plez, B. 1998, A&A, 330, 1109
Aufdenberg, J. P., Hauschildt, P. H., Sankrit, R., & Baron, E. 1999, MNRAS, 302, 599
Aufdenberg, J. P., Hauschildt, P. H., Shore, S. N., & Baron, E. 1998, ApJ, 498, 837
Baraffe, I., Chabrier, G., Allard, F., & Hauschildt, P. H. 1995, ApJ, 446, L35
———. 1997, A&A, 327, 1054
———. 1998, A&A, 337, 403
Baron, E., & Hauschildt, P. H. 1998, ApJ, 495, 370
Brett, J. M. 1990, A&A, 231, 440 (B90)
———. 1995, A&A, 295, 736
Collins, J. G. 1975, J. Phys. B, 8, 304
Collins, J. G., & Faÿ, T. D. J. 1974, J. Quant. Spectrosc. Radiat. Transfer, 14, 1259
Davis, S., Littleton, J., & Phillips, J. 1986, ApJ, 309, 449 (DLP86)
Hauschildt, P. H., Allard, F., & Baron, E. 1999a, ApJ, 512, 377
Hauschildt, P., Allard, F., Ferguson, J., Baron, E., & Alexander, D. R. 1999b, ApJ, 525, 871
Hauschildt, P. H., & Baron, E. 1999, J. Comput. Appl. Math., 102, 41
Hauschildt, P. H., Baron, E., & Allard, F. 1997, ApJ, 483, 390
Hedgecock, L. M., Naulin, C., & Costes, M. 1995, A&A, 304, 667 (HNC95)
Irwin, A. W. 1988, A&AS, 74, 145
Jones, H. R. A., Longmore, A. J., Allard, F., & Hauschildt, P. H. 1996, MNRAS, 280, 77
Jørgensen, U. G. 1994, A&A, 284, 179 (J94)
Jørgensen, U. G., Jensen, P., & Sørensen, G. O. 1994, in IAU Colloq. 146, Molecular Opacities in the Stellar Environment, ed. P. Thejll & U. Jørgensen (Copenhagen: Niels Bohr Inst.), 51
Kirkpatrick, J. D., Kelly, D. M., Rieke, G. H., Liebert, J., Allard, F., & Wehrse, R. 1993, ApJ, 402, 643
Kurucz, R. L. 1993, Kurucz CD-ROM 15, Molecular Data for Opacity Calculations (Cambridge: SAO)
Langhoff, S. R. 1997, ApJ, 481, 1007 (L97)
Leggett, S. K. 1992, ApJS, 82, 351
Leggett, S. K., Allard, F., Berriman, G., Dahn, C. C., & Hauschildt, P. H. 1996, ApJS, 104, 117
Leggett, S. K., Allard, F., Dahn, C., Hauschildt, P. H., Kerr, T. H., & Rayner, J. 2000, ApJ, 535, 965
Leggett, S. K., Allard, F., & Hauschildt, P. H. 1998, ApJ, 509, 836
Leinert, C., Allard, F., Richichi, A., & Hauschildt, P. H. 2000, A&A, 353, 691
Ludwig, C. B. 1971, Appl. Opt., 10, 5, 1057
Miller, S., Tennyson, J., Jones, H. R. A., & Longmore, A. J. 1994, in IAU Colloq. 146, Molecules in the Stellar Environment, ed. U. G. Jørgensen (Berlin: Springer), 296
Partridge, H., & Schwenke, D. W. 1997, J. Chem. Phys., 106, 4618
Plez, B. 1992, A&AS, 94, 527
———. 1998, A&A, 337, 495
Schryber, H., Miller, S., & Tennyson, J. 1995, J. Quant. Spectrosc. Radiat. Transfer, 53, 373
Schwenke, D. W. 1998, Faraday Discuss., 109, 321
Valenti, J. A., Piskunov, N., & Johns-Krull, C. M. 1998, ApJ, 498, 851